Journal of Organometallic Chemistry 695 (2010) 850–862

Contents lists available at ScienceDirect

Journal of Organometallic Chemistry

journal homepage: www.elsevier.com/locate/jorganchem

Syntheses, solid-state structures, solution behavior of hypervalent organobismuth(III) compounds $[2\text{-}(Et_2NCH_2)C_6H_4]_nBiX_{3-n}$ and DFT characterization of $[2\text{-}(Me_2NCH_2)C_6H_4]_nBiX_{3-n}$ [X = Cl, Br, I; n = 1–3]

Albert Soran [a], Hans J. Breunig [b], Vito Lippolis [c], Massimiliano Arca [c], Cristian Silvestru [a,*]

[a] Faculty of Chemistry and Chemical Engineering, "Babes-Bolyai" University, RO-400028 Cluj-Napoca, Romania
[b] Institut für Anorganische und Physikalische Chemie, Universität Bremen, D-28334 Bremen, Germany
[c] Dipartimento di Chimica Inorganica ed Analitica, Università degli Studi di Cagliari, S.S. 554 Bivio per Sestu, 09042 Monserrato (CA), Italy

ARTICLE INFO

Article history:
Received 11 November 2009
Received in revised form 29 December 2009
Accepted 4 January 2010
Available online 11 January 2010

Keywords:
Bismuth
Hypervalent
Halides
X-ray diffraction
Supramolecular
DFT calculations

ABSTRACT

The reaction of RLi [R = 2-$(Et_2NCH_2)C_6H_4$] with $BiCl_3$ in 3:1 or 2:1 molar ratio afforded R_3Bi (**1**) and R_2BiCl (**2**), respectively. Redistribution reactions between **1** and $BiCl_3$ (1:2 molar ratio) resulted in $RBiCl_2$ (**5**). R_2BiBr (**3**) formed from RMgBr and $BiCl_3$ (2:1 molar ratio). R_2BiI (**4**) and $RBiX_2$ [X = Br (**6**), I (**7**)] were obtained from **2** and **5** by halogen-exchange reactions using KX in water/CH_2Cl_2 mixture. Compounds **1**–**7** were characterized by FT-Raman/IR, ^1H and ^{13}C NMR spectroscopies as well as mass spectrometry. The structures of **1**–**4** were determined by single-crystal X-ray diffraction. They all have pyramidal C_3Bi or C_2BiX cores. For R_3Bi (**1**) intramolecular N → Bi interactions of medium strength [Bi(1)–N(1) 3.214(7) Å] result in an overall distorted octahedral $(C,N)_3Bi$ core. In the monohalides **2**–**4** one nitrogen is strongly coordinated to bismuth *trans* to the halogen [range 2.571(8)–2.645(6) Å], while the second one is involved in a considerably weaker intramolecular N → Bi interaction *trans* to a carbon atom [range 2.992(12)–3.170(8) Å]. The overall $(C,N)_2BiX$ (X = Cl, Br, I) core is distorted square-pyramidal. The NMR studies provided evidence for the presence of internal nitrogen-bismuth coordination in solution for $RBiX_2$ species. DFT calculations were performed on the related compounds $R'BiX_2$ [X = Cl (**8**), Br (**9**), and I (**10**)], R'_2BiX [X = Cl (**11**), Br (**12**), and I (**13**)], and R'_3Bi (**14**) [R′ = 2-$(Me_2NCH_2)C_6H_4$] in order to elucidate the bond nature and vibrational spectroscopic features of this class of organobismuth(III) compounds.

1. Introduction

Organobismuth compounds are important in many fields of research [1–8]. As a consequence of the weakness of the Bi–C bond and the pronounced Lewis acidity of Bi(III) compounds many bismuthanes are very sensitive compounds and scrambling reactions with migration or loss of the organic substituents occur frequently. Therefore, rational syntheses are difficult in organobismuth chemistry. Recent developments show that these difficulties can be overcome at least partially by two strategies. One is the use of bulky substituents such as $(Me_3Si)_2CH$ [9–14], 2,6-$R_2C_6H_3$ (R = Mes [15–19], 2,6-$^iPr_2C_6H_3$ [18]), 2,4,6-$R_3C_6H_2$ [$(Me_3Si)_2CH$ [20–21], Ph [22,23]], 2,6-$[(Me_3Si)_2CH]_2$-4-$(Me_3Si)_3C$–C_6H_2 [24–27], 2,6-Mes_2-4-^{t}Bu-C_6H_2 [19]. Another strategy is to use one pendant arm ligands such as 2-$(MeOCR_2)C_6H_4$ (R = Me [28–30], CF_3 [31]) and 2-$(Me_2NCH_2)C_6H_4$ [32], or "pincer" ligands like 2,6-$(Me_2NCH_2)_2C_6H_3$ [32,33], 2,6-$[MeN(CH_2CH_2)_2NCH_2]_2C_6H_3$ [33], and 2,6-$(ROCH_2)_2C_6H_3$ (R = Me [34], ^{t}Bu [34,35]). These ligands protect the bismuth center not only sterically by increased coordination, but also reduce considerably the Lewis acidity which may lead to undesired reactions. A particularly useful ligand combining feasibility with effective protection is the 2-dimethylaminomethylphenyl group, 2-$(Me_2NCH_2)C_6H_4$ [32], and unusual compounds such as the low-valent species *cyclo*-R_4Bi_4 and R_4Bi_2 [36], the first functionalized organobismuth(III) derivatives of the type $RBiCl[(XPR^a_2)(YPR^b_2)N]$ (X, Y = O, S, Se; R^a, R^b = Me, Ph) [37], a compound which exhibits the first metallophilic $Au^I\cdots Bi^{III}$ closed-shell interaction, i.e., $R_2BiAu(C_6F_5)_2$ [38], and species of the type R_2BiOH, $(R_2Bi)_2CO_3$ or *cyclo*-$(RBiS)_2[W(CO)_5]_2$ [32], were synthesized with this substituent.

With the aim to increase the basicity of the coordinating amine group and the sterical protection we have used now the diethylaminomethylphenyl group, 2-$(Et_2NCH_2)C_6H_4$, as one pendant arm ligand capable to coordinate through the *ortho* carbon atom of the phenyl group and the nitrogen of the diethylamino group

* Corresponding author. Tel.: +40 264 593 833; fax: +40 264 590818 (C. Silvestru); +49 421 218 4042 (H.J. Breunig), +39 070 675 4456 (V. Lippolis).
E-mail addresses: hbreunig@uni-bremen.de (H.J. Breunig), lippolis@unica.it (V. Lippolis), cristi@chem.ubbcluj.ro (C. Silvestru).

0022-328X/$ - see front matter © 2010 Elsevier B.V. All rights reserved.
doi:10.1016/j.jorganchem.2010.01.004

and report here the syntheses, structures and spectroscopic properties of compounds R_3Bi (**1**), R_2BiX [X = Cl (**2**), Br (**3**), I (**4**)] and $RBiX_2$ [X = Cl (**5**), Br (**6**), I (**7**)].

2. Results and discussion

2.1. Preparation

Compounds **1** and **2** were obtained by metathesis between the organolithium derivative and $BiCl_3$, in the appropriate molar ratio (Scheme 1). The chloride **5** was obtained by redistribution, starting from **1**. The monoiodide **4** and the dihalides **6** and **7** were obtained from **2** and **5**, respectively, by halide exchange reactions using an excess of the appropriate potassium halide in CH_2Cl_2/water or Et_2O/water mixtures. The bromide **3** was isolated during the attempted synthesis of **1** using the corresponding organomagnesium bromide, due to poor stoichiometry control and *in situ* halide exchange between **2** and the inorganic magnesium salt.

All new compounds are air stable solids. The triorganobismuth **1** and the monohalides **2**–**4** are soluble in common organic solvents, while the dihalides **5**–**7** are well soluble only in DMSO.

2.2. Crystal and molecular structure of [2-(Et_2NCH_2)C_6H_4]$_3$Bi (**1**) and [2-(Et_2NCH_2)C_6H_4]$_2$BiX [X = Cl (**2**), Br (**3**), I (**4**)]

Single crystals suitable for X-ray diffraction were obtained after slow evaporation from diethyl ether solution for **1**, by slow diffusion of *n*-hexane into a CH_2Cl_2 solution for **2** and **4**, while crystals of **3** were obtained by cooling at −28 °C a concentrated diethyl ether solution. Attempts to grow crystals for compound **5**–**7** from common organic solvents failed.

The molecular structure of **1** is depicted in Fig. 1 and selected interatomic distances and angles are listed in Table 1.

The crystal, belonging to the *P*a-3 cubic system, contains highly symmetric discrete molecules which can be generated crystallographically from the asymmetric unit fragment [2-(Et_2NCH_2)-C_6H_4]Bi. The nitrogen atoms coordinate weakly to bismuth [Bi(1)–N(1) 3.214(7) Å; c.f. the sum of covalent and van der Waals radii for nitrogen and bismuth, Σr_{cov}(Bi,N) 2.27 Å and Σr_{vdW}(Bi,N) 3.94 Å] [39] almost *trans* to a Bi–C bond [N(1)–Bi(1)–C(1a) 158.5(2)°]. The Bi–N bond length is considerably longer than those reported for the related [2-(Me_2NCH_2)C_6H_4]$_3$Bi [Bi–N 3.04(2)–3.11(3) Å] [40], a behavior which can be attributed to the combined electronic and steric effects of the ethyl groups on nitrogen. The coordination geometry at bismuth, considering the N → Bi interactions, is distorted octahedral [(*C*,*N*)$_3$Bi core], mainly due to the restrictions imposed by the chelate rings. Thus compound **1** can be described as a hypervalent 14-Bi-6 species [41,42].

The C_3BiN chelate ring is not planar, the nitrogen atom being 1.093 Å out of the best plane defined through the residual C_3Bi unit. This induces planar chirality (with the aromatic ring and the nitrogen atom as chiral plane and pilot atom, respectively; isomers given as S_N and R_N) [43] and indeed the crystal of **1** contains a 1:1 mixture of (*all*-S_N) (Fig. 1) and (*all*-R_N) isomers.

In order to reveal the effect produced by replacing the methyl by ethyl groups on the nitrogen in the pendant arm the monohalides **2**–**4** were also investigated by single-crystal X-ray diffraction studies.

The crystal of chloride **2** contains one independent molecule in the asymmetric unit, while the bromide **3** and the iodide **4** crystallize with three and two independent, quite similar, molecules, respectively, in the unit cell. The molecular structures are shown in Figs. 2–4 and selected interatomic distances and angles are listed in Tables 2 and 3.

The molecular structures of the monohalides **2**–**4** are very similar to those reported for the related [2-(Me_2NCH_2)C_6H_4]$_2$BiX (X = Cl [44], Br, I [32]). A common feature is that both nitrogen atoms of a molecular unit are involved in internal N → Bi interactions of different strength. A strong intramolecular N → Bi interaction is established *trans* to the halogen atom [2.645(6) Å in **2**; 2.614(6)/2.613(6)/2.589(6) Å in **3a**/**3b**/**3c**; 2.627(8)/2.571(8) Å in **4a**/**4b**], consistent with the higher electronegativity of the *trans* atom. The nitrogen atom of the other amine group exhibits a weaker intramolecular interaction [3.056(7) Å in **2**; 3.150(5)/3.085(8)/3.170(8) Å in **3a**/**3b**/**3c**; 2.992(12)/3.122(12) Å in **4a**/**4b**] and its vector lies approximately *trans* to a carbon atom. The strength of the N → Bi interaction *trans* to the halogen atom in the monohalides **2**–**4** is weaker than in [2-(Me_2NCH_2)C_6H_4]$_2$BiX [2.570(5), 2.534(5), and 2.514(4) Å for X = Cl [44], Br, and I [32], respectively], a behavior which is due to combined electronic and steric effects induced by bulkier ethyl groups. The N → Bi interaction *trans* to the carbon atom is of the same magnitude as in [2-(Me_2NCH_2)-C_6H_4]$_2$BiX [3.047(5), 3.151(5) and 3.148(3) Å for X = Cl [44], Br, and I [32], respectively], but however considerably stronger than in the triorganobismuthane **1** [3.214(7) Å]. Taking into account both intramolecular N → Bi interactions *per* metal atom, the overall coordination geometry is distorted square-pyramidal [(*C*,*N*)$_2$BiX cores; hypervalent 12-Bi-5 species [41,42]], a carbon atom in apical position.

The bismuth-halogen bond lengths in [2-(Et_2NCH_2)C_6H_4]$_2$BiX, i.e., Bi–Cl 2.602(2) Å in **2**, Bi–Br 2.7517(10)/2.7484(10)/

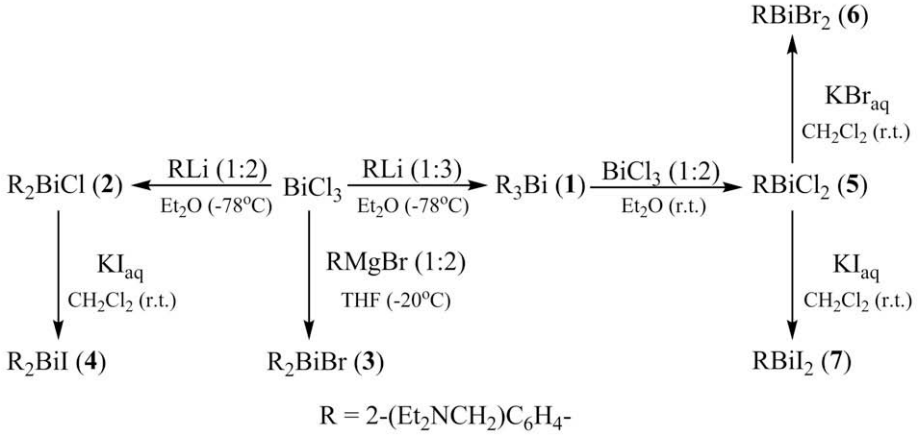

Scheme 1.

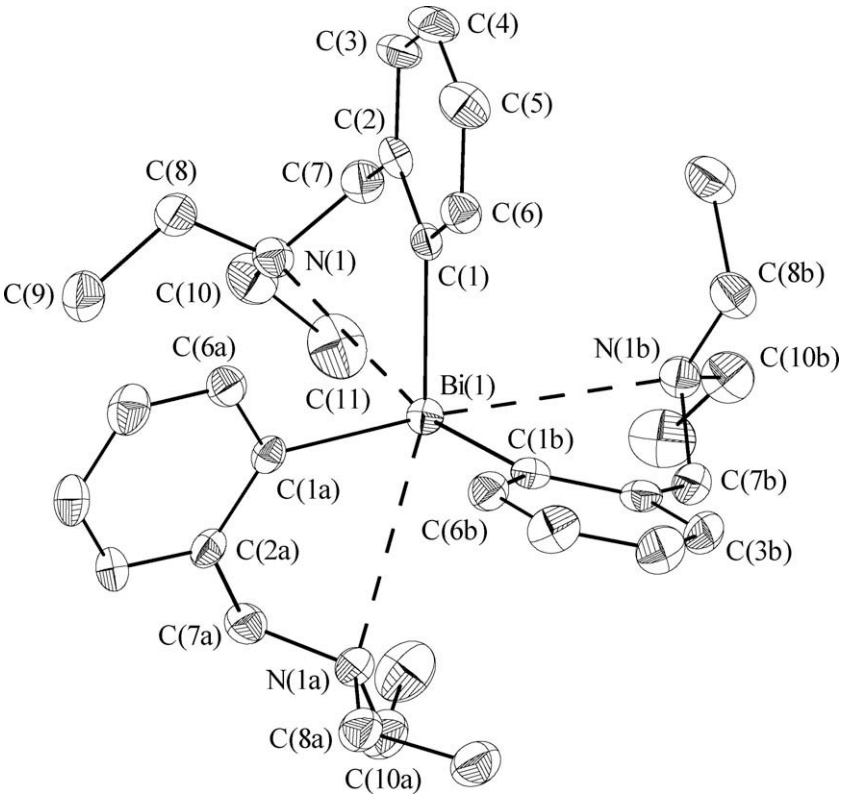

Fig. 1. ORTEP representation at 30% probability and atom numbering scheme for the (*all-S*$_N$)-**1** isomer [symmetry equivalent atoms (z, x, y) and (y, z, x) are given by "a" and "b"; hydrogen atoms are omitted for clarity].

Table 1
Selected bond distances [Å] and angles [°] for compound **1**.[a]

Bi(1)–C(1)	2.271(7)	C(1)–Bi(1)–C(1a)	93.0(3)
Bi(1)–N(1)	3.214(7)	N(1)–Bi(1)–C(1)	66.0(2)
		N(1)–Bi(1)–C(1a)	83.9(2)
N(1)–C(7)	1.455(10)	N(1)–Bi(1)–C(1b)	158.5(2)
N(1)–C(8)	1.463(11)	N(1)–Bi(1)–N(1a)	113.8(2)
N(1)–C(10)	1.479(11)	Bi(1)–N(1)–C(7)	84.4(4)

[a] Symmetry equivalent atoms are given by "a" (z, x, y) and "b" (y, z, x).

2.8084(11) Å in **3a**/**3b**/**3c**, and Bi–I 3.0274(11)/3.0207(10) Å in **4a**/**4b**, are slightly shorter than in the related [2-(Me_2NCH_2)C_6H_4]$_2$BiX [2.667(2), 2.8452(7), and 3.0723(6) Å for X = Cl [44], Br, and I [32], respectively], but longer than those observed in [2,4,6-(CF_3)-C_6H_2]$_2$BiCl [2.463(3) Å] [45], Mes_2BiBr [2.696(2) Å] [46] or [Ph_2BiI(4-Mepy)] [3.0229(8) Å] [47]. This elongation is apparently a consequence of the coordination of the amino group *trans* to the halogen atom.

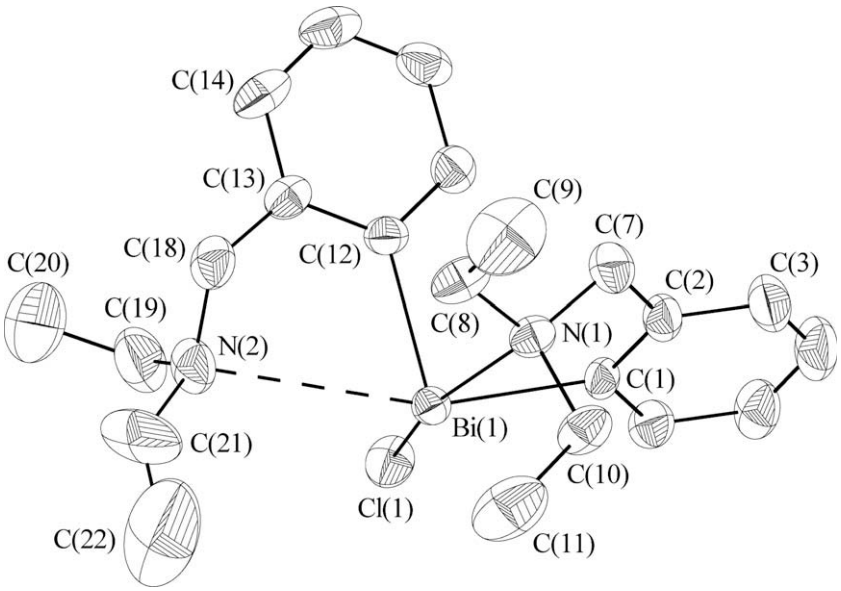

Fig. 2. ORTEP representation at 30% probability and atom numbering scheme for the (S_{N1},R_{N2})-**2** isomer (hydrogen atoms are omitted for clarity).

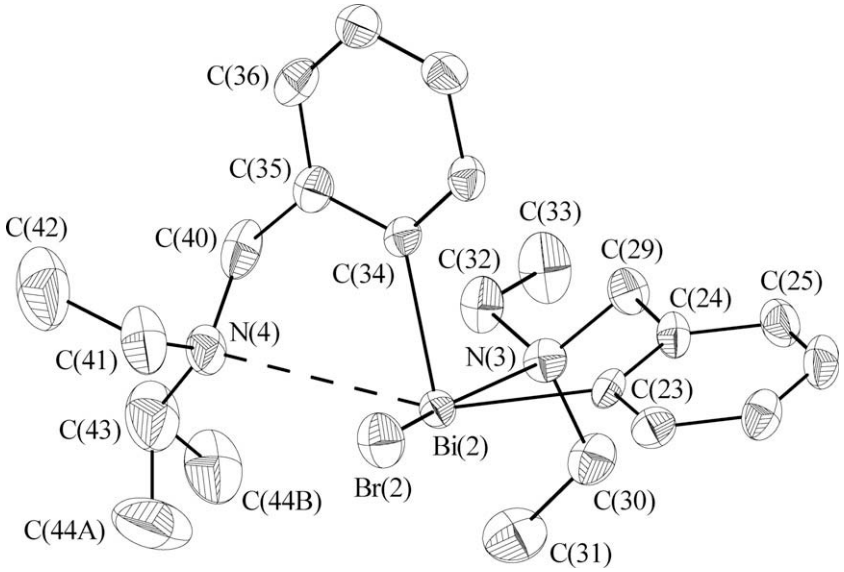

Fig. 3. ORTEP representation at 30% probability and atom numbering scheme for the (R_{N3},S_{N4})-**3b** isomer (hydrogen atoms are omitted for clarity).

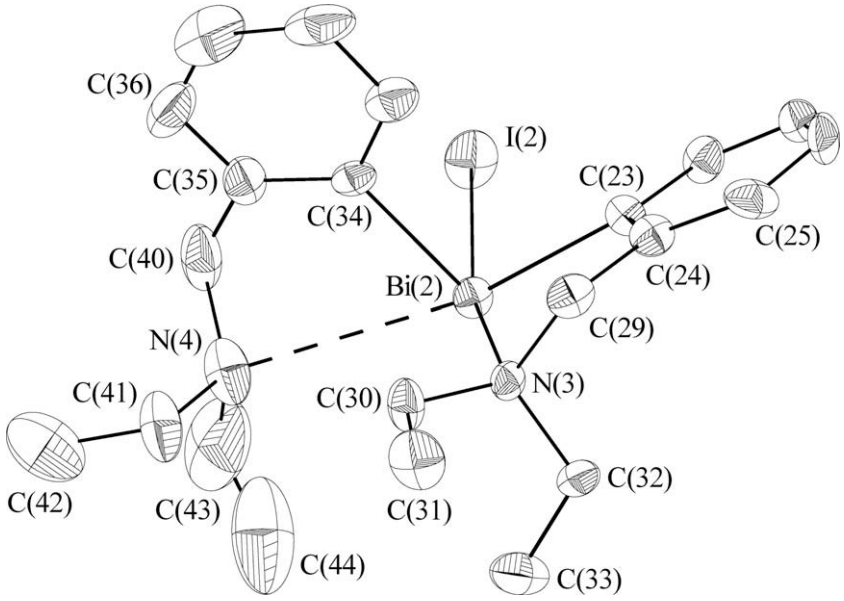

Fig. 4. ORTEP representation at 30% probability and atom numbering scheme for the (S_{N3},S_{N4})-**4b** isomer (hydrogen atoms are omitted for clarity).

As for **1**, the C_3BiN chelate rings in the monohalides **2**–**4** are not planar [distance from nitrogen atom to the best plane of the residual C_3Bi unit: N(1)/N(2) −0.744/0.955 Å in **2**; N(1)/N(2) 0.749/–1.023 Å, N(3)/N(4) 0.773/0.950 Å, and N(5)/N(6) −0.772/−1.200 Å in **3a**, **3b**, and **3c**; N(1)/N(2) 0.680/0.795 Å, N(3)/N(4) −0.586/1.000 Å in **4a** and **4b**]. This induces planar chirality [43] and the crystals of **2** and **3** contain a 1:1 mixture of (S_{N1},R_{N2})/(R_{N1},S_{N2})-**2** isomers and (S_{N1},R_{N2})/(R_{N1},S_{N2})-**3a**, (R_{N3},S_{N4})/(S_{N3},R_{N4})-**3b**, and (S_{N5},R_{N6})/(R_{N5},S_{N6})-**3c** isomers, respectively. The iodide **4** crystallizes in the chiral space group $P2_12_12_1$ (orthorhombic) and therefore the investigated crystal contains only the (S_{N1},R_{N2})-**4a** and (S_{N3},S_{N4})-**4b** isomers.

A closer check of the crystal packing of monohalides **2**–**4** revealed that no intermolecular contacts between heavy atoms are established. However, in addition to intramolecular contacts between halogen and hydrogen atoms (see Supplementary material), there are also intermolecular X···H (X = Cl, Br, I) contacts shorter than the sum of corresponding van der Waals radii [Σr_{vdW}(Cl,H) ca. 3.0 Å, Σr_{vdW}(Br,H) ca. 3.15 Å, Σr_{vdW}(I,H) ca. 3.35 Å] [39], which result in supramolecular associations. Thus, the crystal of **2** contains parallel chain polymers of (S_{N1},R_{N2})-**2** and (R_{N1},S_{N2})-**2** isomers, respectively, established through weak Cl···H_{methyl} contacts [Cl(1)···H(11Bb) 2.91 Å] (Fig. 5). No further contacts are established between the polymeric chains.

The crystal of **4** contains a related polymeric chain built from (S_{N3},S_{N4})-**4b** isomers connected through two weak I···$H_{methylene}$ contacts [I(2)···H(32Aa) 3.07 Å, I(2)···H(29Aa) 3.29 Å]. Each I(2) atom has an additional loose contact [I(2)···H(5d) 3.35 Å], at the limit of the sum of van der Waals radii, with an aromatic proton of an (S_{N1},R_{N2})-**4a** isomer which iodine atom is not involved in any other intermolecular contact (see Supplementary material).

Hexameric aggregates were found in the crystal of **3**. They are built from pairs of (S_{N1},R_{N2})/(R_{N1},S_{N2})-**3a**, (R_{N3},S_{N4})/(S_{N3},R_{N})$_4$-**3b**, and (S_{N5},R_{N6})/(R_{N5},S_{N6})-**3c** isomers. In this case the bromine atoms

Table 2
Selected bond distances [Å] and angles [°] for compounds **2** and **4**.

2		**4a**		**4b**	
Bi(1)–C(1)	2.250(7)	Bi(1)–C(1)	2.281(9)	Bi(2)–C(23)	2.268(11)
Bi(1)–C(12)	2.254(7)	Bi(1)–C(12)	2.249(9)	Bi(2)–C(34)	2.268(11)
Bi(1)–Cl(1)	2.602(2)	Bi(1)–I(1)	3.0274(11)	Bi(2)–I(2)	3.0207(10)
Bi(1)–N(1)	2.645(6)	Bi(1)–N(1)	2.627(8)	Bi(2)–N(3)	2.571(8)
Bi(1)–N(2)	3.056(7)	Bi(1)–N(2)	2.992(12)	Bi(2)–N(4)	3.122(12)
C(1)–Bi(1)–C(12)	93.0(3)	C(1)–Bi(1)–C(12)	94.5(4)	C(23)–Bi(2)–C(34)	95.0(4)
C(1)–Bi(1)–Cl(1)	90.3(2)	C(1)–Bi(1)–I(1)	93.3(3)	C(23)–Bi(2)–I(2)	93.8(3)
C(12)–Bi(1)–Cl(1)	92.3(2)	C(12)–Bi(1)–I(1)	92.5(3)	C(34)–Bi(2)–I(2)	89.8(3)
N(1)–Bi(1)–Cl(1)	161.76(16)	N(1)–Bi(1)–I(1)	165.15(19)	N(3)–Bi(2)–I(2)	166.28(19)
N(1)–Bi(1)–C(1)	71.5(2)	N(1)–Bi(1)–C(1)	72.0(3)	N(3)–Bi(2)–C(23)	72.9(3)
N(1)–Bi(1)–C(12)	87.2(2)	N(1)–Bi(1)–C(12)	86.7(3)	N(3)–Bi(2)–C(34)	88.3(3)
N(1)–Bi(1)–N(2)	110.7(2)	N(1)–Bi(1)–N(2)	99.8(3)	N(3)–Bi(2)–N(4)	94.7(3)
N(2)–Bi(1)–C(1)	159.5(2)	N(2)–Bi(1)–C(1)	160.5(3)	N(4)–Bi(2)–C(23)	157.9(3)
N(2)–Bi(1)–C(12)	67.1(3)	N(2)–Bi(1)–C(12)	67.0(3)	N(4)–Bi(2)–C(34)	65.8(4)
N(2)–Bi(1)–Cl(1)	85.7(2)	N(2)–Bi(1)–I(1)	93.6(3)	N(4)–Bi(2)–I(2)	96.8(2)
Bi(1)–N(1)–C(7)	101.0(5)	Bi(1)–N(1)–C(7)	102.0(6)	Bi(2)–N(3)–C(29)	104.9(6)
Bi(1)–N(2)–C(18)	90.7(5)	Bi(1)–N(2)–C(18)	96.6(7)	Bi(2)–N(4)–C(40)	86.6(8)

Table 3
Selected bond distances [Å] and angles [°] for compound **3**.

3a		**3b**		**3c**	
Bi(1)–C(1)	2.268(8)	Bi(2)–C(23)	2.246(7)	Bi(3)–C(45)	2.230(8)
Bi(1)–C(12)	2.233(7)	Bi(2)–C(34)	2.232(7)	Bi(3)–C(56)	2.244(10)
Bi(1)–Br(1)	2.7517(10)	Bi(2)–Br(2)	2.7484(10)	Bi(3)–Br(3)	2.8084(11)
Bi(1)–N(1)	2.614(6)	Bi(2)–N(3)	2.613(6)	Bi(3)–N(5)	2.589(6)
Bi(1)–N(2)	3.150(5)	Bi(2)–N(4)	3.085(8)	Bi(3)–N(6)	3.170(8)
C(1)–Bi(1)–C(12)	93.0(3)	C(23)–Bi(2)–C(34)	92.6(3)	C(45)–Bi(3)–C(56)	93.2(4)
C(1)–Bi(1)–Br(1)	92.0(2)	C(23)–Bi(2)–Br(2)	90.73(18)	C(45)–Bi(3)–Br(3)	92.2(2)
C(12)–Bi(1)–Br(1)	93.16(18)	C(34)–Bi(2)–Br(2)	88.89(17)	C(56)–Bi(3)–Br(3)	92.4(2)
N(1)–Bi(1)–Br(1)	162.24(14)	N(3)–Bi(2)–Br(2)	162.45(14)	N(5)–Bi(3)–Br(3)	161.97(15)
N(1)–Bi(1)–C(1)	70.7(3)	N(3)–Bi(2)–C(23)	72.2(2)	N(5)–Bi(3)–C(45)	72.8(3)
N(1)–Bi(1)–C(12)	91.6(2)	N(3)–Bi(2)–C(34)	88.0(2)	N(5)–Bi(3)–C(56)	98.1(3)
N(1)–Bi(1)–N(2)	113.3(2)	N(3)–Bi(2)–N(4)	104.7(2)	N(5)–Bi(3)–N(6)	100.1(2)
N(2)–Bi(1)–C(1)	158.2(2)	N(4)–Bi(2)–C(23)	159.2(2)	N(6)–Bi(3)–C(45)	156.9(3)
N(2)–Bi(1)–C(12)	65.9(2)	N(4)–Bi(2)–C(34)	66.6(3)	N(6)–Bi(3)–C(56)	65.6(3)
N(2)–Bi(1)–Br(1)	84.2(1)	N(4)–Bi(2)–Br(2)	89.9(2)	N(6)–Bi(3)–Br(3)	97.6(1)
Bi(1)–N(1)–C(7)	101.6(4)	Bi(2)–N(3)–C(29)	100.3(4)	Bi(3)–N(5)–C(51)	99.8(5)
Bi(1)–N(2)–C(18)	86.6(4)	Bi(2)–N(4)–C(40)	90.1(5)	Bi(3)–N(6)–C(62)	81.5(5)

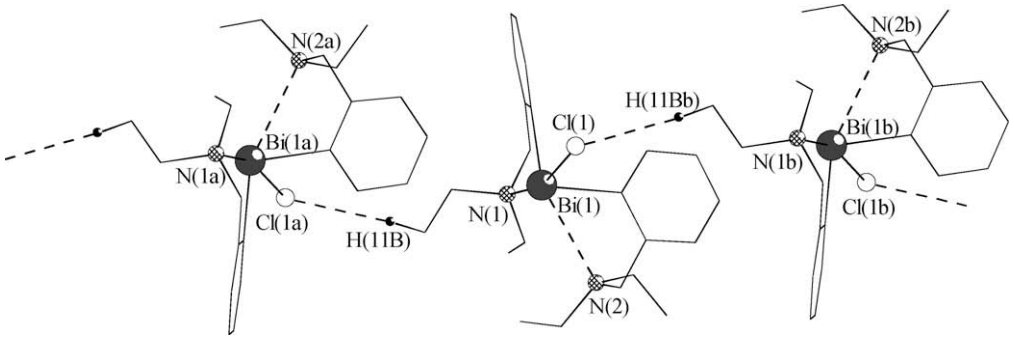

Fig. 5. View of a chain polymer based on Cl···H contacts between (S_{N1},R_{N2}) isomers in the crystal of **2** (only hydrogens involved in intermolecular contacts are shown) [symmetry equivalent atoms (0.5 − *x*, 0.5 + *y*, 1.5 − *z*) and (0.5 − *x*, −0.5 + *y*, 1.5 − *z*) are given by "a" and "b", respectively].

also exhibit different connectivity with hydrogen atoms, i.e.: Br(1) and Br(2) atoms are involved in intermolecular contacts with hydrogen atoms [Br(1)···H(53Ba)$_{methyl}$ 3.01 Å, Br(2)···H(11B)$_{methyl}$ 3.03 Å; Br(2)···H(54Ac)$_{methylene}$ 3.13 Å, Br(2)···H(55Bc)$_{methyl}$ 3.04 Å], while Br(3) is not involved in any other intermolecular contact (see Supplementary material).

2.3. NMR spectra

The assignment of the signals in the room temperature ^{1}H and ^{13}C NMR spectra of compounds **1**–**7** was based on the 2D NMR spectra according to the numbering scheme shown in Scheme 2.

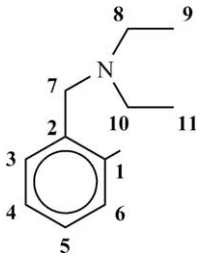

Scheme 2.

The ^{1}H NMR spectra (in $CDCl_3$) of the bismuthane **1** and the monohalides **2–4** show, besides one singlet for the benzylic protons, a triplet and a quartet resonance for the ethyl groups in the aliphatic region and one set of aromatic resonances, respectively, thus indicating equivalence of the organic groups attached to the metal atom. This is consistent with either the absence of N → Bi coordination or rapid nitrogen inversion. A similar behavior was observed for the related bismuthane [2-(Me_2NCH_2)C_6H_4]$_3$Bi [40] and is expected for non-metallochiral bismuthanes. In contrast, the room temperature ^{1}H NMR spectra of the dihalides **5–7** show besides one triplet for the methyl protons of the ethyl groups and one singlet for the benzylic protons, an apparently complex pattern for the methylene protons of the ethyl groups. This pattern was interpreted and was confirmed by simulation to be an AB system composed of two doublets of quartets. A possible explanation for the appearance of the ^{1}H NMR spectra of **5–7** is that the nitrogen–bismuth interaction is preserved in solution, which would also be consistent with the higher Lewis acidity of bismuth in comparison with the corresponding halodiorganobismuthines **2–4**. Although the two ethyl groups are equivalent due to the fact that the nitrogen atom can coordinate to bismuth *trans* to any of the two halogen atoms with equal chance, the two methylene hydrogen atoms within each ethyl group are diastereotopic. In the absence of the N–Bi interaction nitrogen inversion would exchange the two ethyl groups and the methylene protons within each ethyl group would be in this case only enantiotopic, as in the free ligand, and thus undistinguishable by NMR. Another possible proof of the existence of N–Bi interaction in solution is that in the case of **5–7** a similar downfield shift as observed for the H_6 proton, is also observed for the benzylic and methylene protons albeit this is not observed in ^{1}H NMR spectra of **2–4**. Although there are no direct evidences (crystals suitable for single-crystal X-ray diffraction could not be obtained), it is very likely that in solid state, due to the higher Lewis acidity of the bismuth atom, the molecules of the dihalides **5–7** are associated through intermolecular Bi···halogen interactions as was found for the related [2-(Me_2NCH_2)C_6H_4]BiX_2 (X = Cl [32], I [44]).

For all compounds formation of the bismuth–carbon bond was confirmed by the downfield shifted resonance of the *ortho* to bismuth aromatic protons (H_6). This shift is increasingly larger when going from the chloro- to the iodo substituted compounds in the series **2–4** or **5–7**. If we compare the chemical shift of the H_6 proton in triorganobismuthine **1**, halodiorganobismuthines **2–4** and dihalorganobismuthines **5–7** it is also obvious that this increases with the increased number of halogen atoms bound to bismuth.

In the ^{13}C NMR spectra the halogen exchange in the compounds **2–4** and **5–7** is mainly reflected in an increased upfield shift of the resonance signal for the aromatic C-1 atom bonded to bismuth, when chlorine is changed by bromine or iodine, respectively. As expected, this trend follows the decrease in electronegativity from Cl to I.

2.4. Theoretical calculations

During the past decades, the analysis of the nature of the bonding systems and of the spectroscopic and electrochemical features of inorganic and organometallic compounds has been largely helped by theoretical calculations carried out at different levels of theory. In recent years, density functional theory (DFT) [48] has been widely acknowledged as a theoretical approach capable of providing very accurate information at acceptable computational costs, *e.g.* evidences for the electronic rather than steric stabilization of the square-pyramidal geometry of bismuth in [2,6-(Me_2NCH_2)$_2C_6H_3$]$BiCl_2$ were confirmed by theoretical calculations [49]. In this context, we recently reported on a hybrid DFT investigation aimed to interpret structural and spectroscopic properties of monoorganobismuth(III) dihalides containing the 2,6-[$MeN(CH_2CH_2)_2NCH_2]_2C_6H_3$ pincer ligand [33]. Prompted by the results achieved, we have now extended to the title compounds DFT calculations carried out at the same theoretical level. As computational models, the compounds belonging to the general classes R′BiX_2 [X = Cl (**8**), Br (**9**), and I (**10**); Scheme 3, a], R′$_2$BiX [X = Cl (**11**), Br (**12**), and I (**13**); Scheme 3 b], and R′$_3$Bi (**14**; Scheme 3 c) have been considered [R′ = 2-(Me_2NCH_2)C_6H_4].

The crystal structures of [2-(Me_2NCH_2)C_6H_4]BiX_2 [X = Cl (**8**) [32], I (**10**) [44]) were recently reported showing the compounds to form discrete centrosymmetric dimers *via* X → Bi interactions. We have therefore optimized the structures of the three monomeric R′BiX_2 compounds **8–10**, and of the corresponding dimers [(**8**)$_2$, (**9**)$_2$, and (**10**)$_2$, respectively] without imposing any constraints, in order to investigate the nature of chemical bond in such systems and verify whether the dimerization found for **8** and **10** could also be predicted for the bromine analogue, **9**, whose crystal structure was not yet determined, as well as for **5–7**. In Table 4 some selected optimized bond distances for **8–10** and (**8**)$_2$–(**10**)$_2$ are summarized and compared to the corresponding parameters determined by X-ray diffraction for (**8**)$_2$ and (**10**)$_2$. The bond distances optimized for (**8**)$_2$ and (**10**)$_2$ are in fairly good agreement with those from the X-ray diffraction analyses. In the monomers **8–10** the two Bi–X(1) and Bi–X(2) distances are calculated to be not equivalent, the Bi–X(2) bond *trans* with respect to the Bi–N one being the longest. On passing from the monomers to the corresponding dimers, both Bi–X distances undergo remarkable elongations, while the Bi–N distances result correspondingly shortened. It is worth underlining that while Bi–C distances are only very marginally affected by the nature of the halogen bonded to the bismuth centers, the Bi–N bond lengths increase systematically with the decreasing electronegativity of the halogen species. This trend is confirmed by Wiberg bond indices (WBI) [50], which show a decrease in the Bi–N bond strengths [0.218, 0.213, and 0.206 for (**8**)$_2$, (**9**)$_2$, and (**10**)$_2$, respectively] and a corresponding increase in the strength of the *trans*-disposed Bi–X bonds [0.406, 0.483, and 0.563 for (**8**)$_2$, (**9**)$_2$, and (**10**)$_2$, respectively] on going from X = Cl to Br and I.

The dimer formation can be split ideally into two subsequent steps: (i) the constraining of geometry of the monomers **8–10** optimized without any constraints to assume that calculated for each unit in the dimers (**8**$_{dim}$–**10**$_{dim}$); (ii) the interaction between two monomer units **8**$_{dim}$–**10**$_{dim}$ to give the dimers (**8**)$_2$–(**10**)$_2$. The MO shapes and the Mulliken charge distributions on the involved atomic species calculated for **8**$_{dim}$–**10**$_{dim}$ (Q_{Bi} = 0.871, 0.776, 0.664 e; $Q_{X(2)}$ = −0.517, −0.461, −0.411 e, for **8**$_{dim}$, **9**$_{dim}$, and **10**$_{dim}$, respectively) allow to consider the dimer formation as a charge-transfer process involving the overlap of the filled frontier molecular orbitals (HOMO-1 for **8**$_{dim}$; HOMO for **9**$_{dim}$ and **10**$_{dim}$), consisting of a np_z lone pair localized on the X(2) atom (n = 3, 4, and 5 for Cl, Br, and I), and the LUMO, which is antibonding-in-nature with respect to the Bi–X(1) bond (Fig. 6), this is in agreement with the trend in the Bi–X distances, mentioned above, and calculated on passing from **8–10** to the corresponding dimers. Notably, a second order perturbation theory analysis of the Fock matrix in the NBO basis (PT2F-NBO) unveils that the entity of the interactions

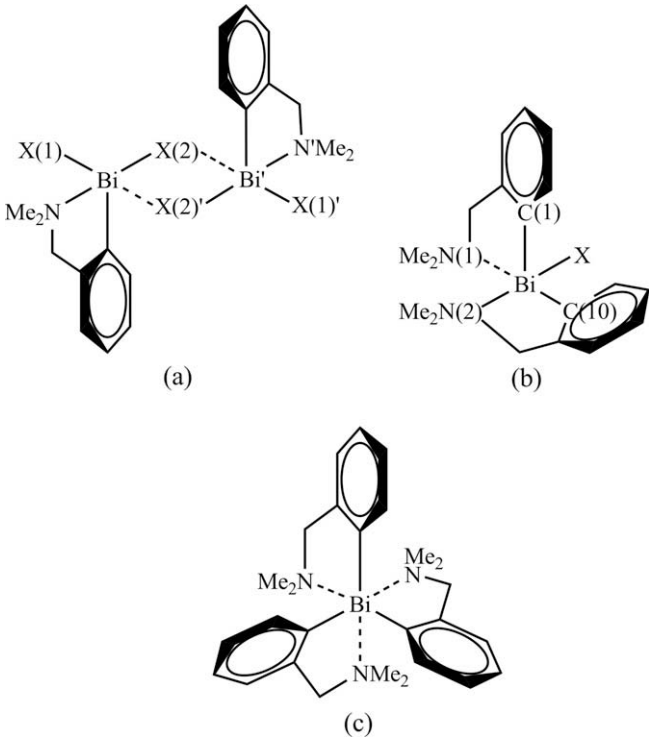

Scheme 3.

between the two units originating the dimers does not vary significantly on passing from X = Cl to I, the interaction energy between the lone pair (LP) natural orbital localized on the bridging halogen of one unit and the bismuth center of the second unit being of 35.5, 29.6, and 29.8 kcal mol^{-1} for (**8**)$_2$, (**9**)$_2$, and (**10**)$_2$, respectively.

Although basis set superposition errors (BSSE) should be taken into account when considering the weak interactions of complex fragments, these corrections have been reported to be negligible within the DFT formalism when triple-ζ BS are used for the heaviest atoms, and for bismuth in particular [51] and are anyway of small entity (less than 2 kcal mol^{-1}) with double-ζ BS, such as LanL2DZ, adopted here for bismuth and for halogen species [52]. Thus, without taking into account counterpoise corrections, a comparison of the total electronic energies (Fig. 7) shows that the geometry distortion occurring on passing from **8**–**10** to **8**$_{dim}$–**10**$_{dim}$ is compensated by the dimer formation, allowing to evaluate in 20.3, 18.0, and 15.2 kcal mol^{-1} the final stabilization energies ΔE obtained on passing from **8**–**10** to (**8**)$_2$–(**10**)$_2$. Therefore, although ΔE slightly decreases on passing from X = Cl to I, it is conceivable to suppose that also **9** and **5**–**7** could form stable dimers *via* X → Bi interactions as found in the case of **8** and **10** in the solid state. Interestingly, the stabilization energy calculated for (**8**)$_2$ is of the same order of magnitude of that found in the case of the monoorganobismuth(III) dichloride of the 2,6-(Me$_2$NCH$_2$)$_2$C$_6$H$_3$ pincer ligand containing a T-shaped CBiCl$_2$ core on passing from one to two N → Bi interactions [49].

The bond distances optimized for diorganobismuth(III) halides R′$_2$BiX (Scheme 3 b; Table 5) show, in agreement with structural data, that the two ligand moieties feature different bond distances at the bismuth center. In particular, while Bi–C bond distances are quite similar to each other [and similar to those calculated for (**8**)$_2$–(**10**)$_2$], the two Bi–N distances differ significantly, the one in *trans* with respect to the halogen atom being shorter. Wiberg bond indexes testify for such difference: WBIs calculated for the shorter Bi–N bonds (0.143, 0.141, and 0.137 for **11**, **12**, and **13**, respectively) are more than double than those calculated for the longer ones (0.066, 0.065, and 0.064 for **11**, **12**, and **13**, respectively). It is worth noting that the Bi–X bonds get stronger on passing from X = Cl to X = I (WBI: 0.594, 0.665, and 0.732 for **11**, **12**, and **13**, respectively). As in the case of (**8**)$_2$–(**10**)$_2$, a PT2F-NBO analysis shows that the interaction of the nitrogen lone pairs to the bismuth center is much stronger when the nitrogen atom is in *trans* to a halogen atom rather than a carbon atom. In fact, such interaction was evaluated to be 28.3, 19.5, and 19.6 kcal mol^{-1} for **11**, **12**, and **13**, respectively, in the former disposition and 5.2, 5.6, and 5.7 kcal mol^{-1} for **11**, **12**, and **13**, respectively, in the latter disposition.

Finally, on passing to the triorganobismuth(III) compound R′$_3$Bi (**14**; Scheme 3 c), the Bi–C bond distance is longer than the Bi–N one in agreement with experimental data. In particular, as expected, the Bi–C distance and the corresponding WBI (2.275 Å and 0.687, respectively) are again similar to those calculated in the case of compounds **8**–**13**. The Bi–N optimized distance (3.032 Å) and the corresponding bond index (0.058) are instead very close to those calculated for **11**–**13** in the situation where the nitrogen atom is not *trans*-disposed with respect to a halogen species [N(1) in Scheme 3 b, for **11**–**13**].

Table 4
Selected bond distances [Å] calculated for **8**–**10** and for the corresponding dimeric units (**8**)$_2$–(**10**)$_2$ (see Supplementary material for optimized geometries in orthogonal Cartesian format).[a]

	X	Bi–X(1)	Bi–X(2)	Bi–X(2)′	Bi–C	Bi–N
8	Cl	2.479	2.523	–	2.233	2.681
9	Br	2.640	2.687	–	2.237	2.700
10	I	2.838	2.889	–	2.242	2.721
(**8**)$_2$	Cl	2.531	2.723	3.014	2.230	2.546
(**8**)$_2$[b]	Cl	2.595(2)	2.825(2)	2.899(2)	2.225(7)	2.458(6)
(**9**)$_2$	Br	2.691	2.887	3.209	2.235	2.568
(**10**)$_2$	I	2.893	3.049	3.442	2.240	2.590
(**10**)$_2$[c]	I	2.987(1)	3.116(1)	3.243(1)	2.239(8)	2.503(6)

[a] Labeling scheme refers to Scheme 3a.
[b] Experimental data from Ref. [32].
[c] Experimental data from Ref. [44].

2.5. Raman vibrational spectroscopy

FT-Raman spectroscopy demonstrated to be of great help in giving qualitative structural information on the nature of the products obtainable by reacting dihalogens and interhalogens with donor molecules containing 15- and 16-group elements in the absence of structural data [53]. In fact, the Raman peaks related to the vibration modes of the halogen-containing frameworks are generally much more intense than those arising from the vibrations of the remaining organic framework, and their position in the spectrum can be related to the structural features of such products. Conscious of the fact that an accurate correlation between structural features and vibrational properties always requires the vibrational analysis of a large number of crystallographically characterized compounds for each structural archetype, we have started a research program to see whether organobismuth(III) halides stabilized by intramolecular N → Bi interactions are characterized by distinctive vibrational properties that could be used to identify their structural nature in the absence of X-ray diffraction data. In this context, we have reported recently on an experimental and theoretical analysis of monoorganobismuth(III) dihalides of the 2,6-[MeN(CH$_2$CH$_2$)$_2$-NCH$_2$]$_2$C$_6$H$_3$ and 2,6-(Me$_2$NCH$_2$)$_2$C$_6$H$_3$ pincer ligands containing a T-shaped CBiX$_2$ core [33], showing how theoretical calculations allowed to interpret vibrational spectra and to recognize the contribution from Bi–C, N–Bi–N, and X–Bi–X discrete fragments (X = halogen). Encouraged by those results, we have now turned to apply DFT calculations to the title mono- and diorganobismuth(III)

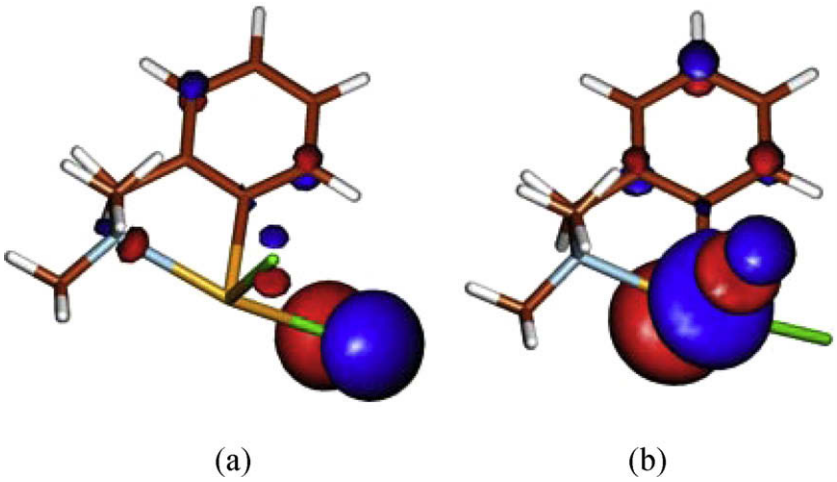

Fig. 6. Drawings of Kohn–Sham HOMO-1 (a) and LUMO (b) calculated for **8**. Contour value 0.05 e.

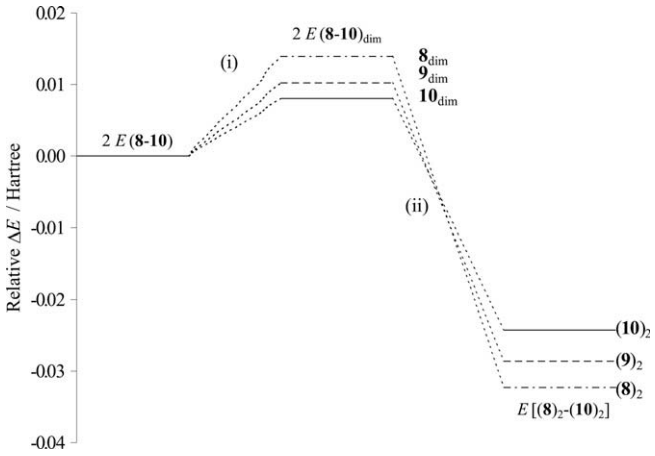

Fig. 7. Total electronic energy stabilization ΔE (Hartree) calculated on passing from **8**–**10** to $(\mathbf{8})_2$–$(\mathbf{10})_2$. All energies are referred to those of each monomer.

Table 5
Selected bond distances [Å] calculated for **11**–**13**,[a] compared with experimental data (see Supplementary material for optimized geometries in orthogonal Cartesian format).

	X	Bi–C(1)	Bi–C(10)	Bi–N(1)	Bi–N(2)	Bi–X
11	Cl	2.255	2.269	2.983	2.695	2.567
11[b]	Cl	2.264(5)	2.258(6)	3.047(5)	2.570(5)	2.667(2)
12	Br	2.254	2.272	3.007	2.705	2.730
12[c]	Br	2.254(6)	2.255(6)	3.151(5)	2.534(5)	2.845(1)
13	I	2.254	2.277	3.030	2.719	2.933
13[c]	I	2.256(4)	2.267(4)	3.148(3)	2.514(4)	3.072(1)

[a] Labeling scheme refers to Scheme 3b.
[b] Experimental data from Ref. [44].
[c] Experimental data from Ref. [32].

halides, to verify whether, in this case also, Raman peaks peculiar of discrete groups containing the halogen atoms could be envisaged. As discussed above, calculations were carried out on compounds belonging to the general classes $[R'BiX_2]_2$ [X = Cl $(\mathbf{8})_2$, Br $(\mathbf{9})_2$, and I $(\mathbf{10})_2$] and R'_2BiX [X = Cl (**11**), Br (**12**), and I (**13**)]. Since alkyl groups affect only marginally the vibration falling in the FIR region (50–500 cm^{-1}), vibrational modes calculated for compounds $(\mathbf{8})_2$–$(\mathbf{10})_2$ and **11**–**13** can be usefully exploited to interpret the spectra of compounds **5**–**7** and **2**–**4**, respectively, containing the ligand 2-$(Et_2NCH_2)C_6H_4$ (see Supplementary material). As previously pointed out, the complexity of the organic frameworks is reflected in complex combinations of normal modes involving Bi–C, Bi–X, and Bi–N vibrators. In the following, only the vibrational modes having the largest contribution from the above mentioned fragments will be considered. The most intense calculated Raman-active vibrational modes are summarized in Table 6.

In both calculated and experimental Raman spectra of the examined compounds $(\mathbf{8})_2$–$(\mathbf{10})_2$, **11**–**13**, the most intense peaks correspond generally to the stretching modes involving the Bi–X bonds. Since bismuth–halogen optimized distances are slightly different from the structural ones (Tables 4 and 5), the corresponding unscaled vibrational frequencies are systematically overestimated. A linear regression holds between the calculated Bi–X Raman-active frequencies and the experimental ones ($R^2 = 0.90$), allowing to evaluate a scaling factor of 0.88, as it could be found in the previous calculations mentioned above [33]. Notably, in $(\mathbf{8})_2$–$(\mathbf{10})_2$, the vibration modes (ν_{Bi-X}) containing the largest contribution from the Bi–X stretching are systematically more energetic than those calculated for **11**–**13**, reflecting the strength of the corresponding bismuth–halogen bonds previously discussed on the bases of the experimental and optimized bond lengths and of the calculated WBIs. As expected, the peaks due to the Bi–X stretching vibrations undergo the most evident shift towards lower energies on passing from X = Cl to X = I for both sets of compounds. A comparison of the calculated ν_{Bi-X} values for $(\mathbf{8})_2$–$(\mathbf{10})_2$, for **11**–**13**, and of the ν_{X-Bi-X} vibrational modes (symmetric and antisymmetric) calculated for monoorganobismuth(III) dihalides of the 2,6-$(Me_2NCH_2)_2C_6H_3$ pincer ligand [33] seems to show that the energy of the corresponding vibrations is related to the number and nature of the N → Bi interactions involved: the highest in the presence of a single N → Bi interaction in $[R'BiX_2]_2$-type compounds like $(\mathbf{8})_2$–$(\mathbf{10})_2$ (see Table 6), the lowest in the presence of two N → Bi interactions in $RBiX_2$-type compounds with pincer-ligands [$\nu^s_{X-Bi-X} = 242$ (Cl); 151 (Br); 101 (I); R = 2,6-$(Me_2NCH_2)_2C_6H_3$] [33]. Therefore, in the absence of structural data FT-Raman spectroscopy could be exploited as a tool to tentatively hypothesize the chemical environment of the Bi(III) center on the basis of the wavenumber of the vibration modes containing the largest contribution from the stretching of Bi–X fragments. A second clearly identifiable set of peaks is that corresponding to the Bi–C stretching modes, falling at about 350 cm^{-1}. These peaks are very marginally affected by the stoichiometry of the compounds and by the number and nature of the halogen ligands.

Table 6
Selected Raman-active frequencies ν (cm^{-1})[a] calculated in the FIR region (50–500 cm^{-1}) for compounds $(\mathbf{8})_2$–$(\mathbf{10})_2$ and **11**–**13**.

Groups[b] Mode	X(1)–Bi–X(2) Bending	Bi–C(Ph)[c] Bending	Bi–X Stretching	C(1)–Bi–C(10) Stretching	Bi–C(1,10) Stretching	Bi–N Stretching
$(\mathbf{8})_2$	77.4	–	282.6	–	353.7	454.8
$(\mathbf{9})_2$	73.6	–	193.3	–	353.1	452.1
$(\mathbf{10})_2$	59.5	–	135.8	–	352.7	449.5
11	–	38.3, 48.5	258.4	190.5	350.1, 357.1	384.9, 420.1[d]
12	–	36.3, 49.8	172.1	190.6	351.1, 356.9	386.0, 413.1[d]
13	–	47.0, 51.5	127.8	189.3	348.3, 354.2	388.1, 413.1[d]

[a] Unscaled harmonic frequencies.
[b] Labeling scheme refers to Scheme 3.
[c] Libration of the phenyl group along the Bi–C bond.
[d] The Bi–N stretching is originated by a torsion of the methylene bridge.

The very good agreement between the Bi–C optimized bond distances and the experimental ones is reflected in calculated frequencies very close to the FT-Raman experimental ones (see Supplementary material).

Finally, the vibrations involving the Bi–N bonds are much more complex. All such vibrational motions are in fact combined with different vibrations of the rest of the organic moiety, as previously found for T-shaped organobismuth(III) dihalides. In all cases anyway, these vibrations are calculated at about 450 cm^{-1} for $(\mathbf{8})_2$–$(\mathbf{10})_2$ and in the range 380–420 cm^{-1} for **11**–**13**. In the experimental Raman spectra these bands are not intense and a confirmation of their position can be looked for in the corresponding FT-IR spectra (see Supplementary material).

3. Conclusions

The replacement of methyl by ethyl groups at the nitrogen atom of the pendant arm in compounds of the type $[2\text{-}(R_2NCH_2)\text{-}C_6H_4]_nBiX_{3-n}$ (n = 1–3) does not affect dramatically the structure. In solid state the monohalides $[2\text{-}(Et_2NCH_2)C_6H_4]_2BiX$ [X = Cl (**2**), Br (**3**), I (**4**)] exhibit two internal N → Bi interactions of different strength. The vector of the weaker one lies approximately *trans* to a carbon atom and is of the same magnitude as in the methyl analogues, but however considerably stronger than in the triorganobismuthane $[2\text{-}(Et_2NCH_2)C_6H_4]_3Bi$ (**1**). The strong N → Bi interaction is established *trans* to the halogen atom and its strength is lower than in the methyl analogues due to combined electronic and steric effects induced by bulkier ethyl groups. Planar chirality is induced due to the folded five-membered BiC_3N rings and the compounds crystallize as racemates. While the crystal of **1** contains discrete molecules, those of the monohalides **2**–**4** contain chain polymer associations (**2** and **4**) or hexameric aggregates built through intermolecular X···H contacts. The room temperature ^1H NMR spectra provided evidence for the presence of internal nitrogen–bismuth coordination in solution for the dihalides $[2\text{-}(Et_2NCH_2)C_6H_4]BiX_2$ [X = Cl (**5**), Br (**6**), I (**7**)]. The use of DFT theoretical calculations allowed to investigate the nature of the chemical bond in the title systems and to study the driving force leading to dimerization in monoorganobismuth(III) dihalides like **8**–**10**. In addition, calculations have been exploited to investigate FT-Raman vibrational spectra in the attempt to find distinctive vibrational features in mono- and diorganobismuth(III) compounds linked to the nature of X → Bi and N → Bi interactions.

4. Experimental

4.1. Materials and procedures

The ^1H, ^{13}C and 2D NMR spectra were recorded at room temperature, in dried $CDCl_3$ (**1**, **2**–**4**) or DMSO-d_6 (**5**–**7**), on Bruker Avance 300 or Bruker Avance DRX 400 instruments. The chemical shifts are reported in ppm relative to the residual peak of the solvent (ref. $CHCl_3$: ^1H 7.26, ^{13}C 77.0 ppm; DMSO-d_5: ^1H 2.50, ^{13}C 39.43 ppm). The NMR spectra were processed using the *MestReC* and *MestReNova* software [54]. Mass spectra were recorded with Finnigan MAT 95 (**1**, **5**, **7**) and Finnigan MAT 8200 (**2**–**4**, **6**) instruments and were processed using the *MASPEC II* software [55]. Infrared spectra were recorded on a Bruker IFS120 HR spectrometer at room temperature, purging the sample cell with a flow of dried air. Polythene pellets with a mylar beam-splitter and polythene windows (500–50 cm^{-1}, resolution 2 cm^{-1}) were used. FT-Raman spectra, in the range 500–50 cm^{-1}, were recorded with a resolution of 2 cm^{-1} on a Bruker RFS100 FT-Raman spectrometer, fitted with an In-Ga-As detector (room temperature) operating with a Nd-YAG laser (excitation wavelength 1064 nm; 100 mW), with a 180° scattering geometry. Elemental analyses were performed by Facultatea de Farmacie, Universitatea de Medicina si Farmacie "Iuliu Hatieganu", Cluj-Napoca (Romania). Melting points were measured on an Electrothermal 9200 apparatus and are not corrected. Compounds **1**–**3** and **5** were prepared under an inert atmosphere of argon (Linde, 99.999%) using Schlenk techniques. Solvents were dried and freshly distilled under argon prior to use. $BiCl_3$ was sublimated at 225 °C under high vacuum and was kept under argon. The $2\text{-}(Et_2NCH_2)C_6H_4Br$ [56,57] and $2\text{-}(Et_2NCH_2)C_6H_4Li$ [56] were prepared according to the published methods. All other reagents were obtained from Aldrich or Merck and were used as received.

4.2. Synthesis of $[2\text{-}(Et_2NCH_2)C_6H_4]_3Bi$ (**1**)

A solution of $BiCl_3$ (2.556 g, 8.1 mmol) in diethyl ether (100 ml) was added during 1 h to a solution of $[2\text{-}(Et_2NCH_2)C_6H_4]Li$ (4.115 g, 24.3 mmol) in diethyl ether (100 ml), kept at −78 °C. The reaction mixture was stirred at this temperature for a further one hour and then overnight during which time it reached room temperature. The reaction mixture was filtered under argon through a glass frit with Celite bed and the clear filtrate was washed with distilled water (100 ml). The organic phase was separated and dried over anhydrous Na_2SO_4. The title compound was obtained as a crystalline white powder after removal of the solvent and recrystallization from diethyl ether. Particularly big, colorless crystals are formed on slow evaporation of a diethyl ether solution of **1**. Compound **1** is soluble in chloroform, methylene chloride, thf, hexane, petroleum ether. Yield: 3.2 g (57%). M.p. 97–98 °C. Anal. Calc. for $C_{33}H_{48}BiN_3$: C, 56.97; H, 6.95; N, 6.04. Found: C, 56.75; H, 6.80; N, 5.84%. ^1H NMR (400 MHz, $CDCl_3$, 27 °C): δ 0.79t (18H, $H_{9,11}$, $^3J_{HH}$ 7.1 Hz), 2.41q (12H, $H_{8,10}$, $^3J_{HH}$ 7.1 Hz), 3.63s (6H, H_7), 7.08t (3H, H_5, $^3J_{HH}$ 7.0 Hz), 7.21t (3H, H_4, $^3J_{HH}$ 7.0 Hz), 7.28d (3H, H_3, $^3J_{HH}$ 7.3 Hz), 7.70d (3H, H_6, $^3J_{HH}$ 7.1 Hz). ^{13}C NMR (100 MHz, $CDCl_3$, 27 °C): δ 9.90 ($C_{9,11}$), 45.02 ($C_{8,10}$), 62.18 (C_7), 126.15 (C_4), 129.04 (C_5), 129.23 (C_3), 140.25 (C_6), 145.37 (C_2), 165.41 (C_1). MS (EI, 70 eV, 196.5 °C): m/z (%) 695 (0.4) [M^+], 694 (1) [M^+−H], 680 (1)

[M^+−Me], 533 (100) [R_2Bi^+], 503 (9) [R_2Bi^+−C_2H_6], 460 (5) [R_2Bi^+−$(C_2H_5)_2NH$], 371 (53) [RBi^+], 370 (84) [RBi^+−H]; 341 (65) [RBi^+−C_2H_6], 299 (65) [RBi^+−$(C_2H_5)_2NH$], 209 (46) [Bi^+], 162 (96) [R^+], 91 (86) [$C_7H_7^+$].

4.3. Synthesis of [2-(Et_2NCH_2)C_6H_4]$_2$BiCl (**2**)

A solution of [2-(Et_2NCH_2)C_6H_4]Li (3.41 g, 20.2 mmol) in diethyl ether (60 ml) was added during 1 h to a solution of $BiCl_3$ (3.18 g, 10.1 mmol) in diethyl ether (80 ml), kept at −78 °C. The reaction mixture was stirred at this temperature for a further one hour and then overnight when it reached room temperature. After filtration through a glass frit with Celite bed, under argon, the solvent was removed in vacuum from the clear filtrate to give an oily residue. Treatment with hexane resulted in deposition of **2** as a white powder, which was filtered off, washed with hexane (2 × 20 ml) and dried (2.36 g, 45%). Compound **2** is soluble in chloroform, methylene chloride, thf and slightly soluble in hexane and petroleum ether. Yield: 2.36 g (45%). M.p. 112 °C. Anal. Calc. for $C_{22}H_{32}BiClN_2$: C, 46.44; H, 5.67; N, 4.92. Found: C, 46.25; H, 5.27; N, 5.18%. ^{1}H NMR (400 MHz, $CDCl_3$, 27 °C): δ 1.02t (12H, $H_{9,11}$, $^3J_{HH}$ 7.1 Hz), 2.69q (8H, $H_{8,10}$, $^3J_{HH}$ 7.1 Hz), 3.86s (4H, H_7), 7.38 m (4H, $H_{4,5}$), 7.52d (2H, H_3, $^3J_{HH}$ 7.3 Hz), 8.56d (2H, H_6, $^3J_{HH}$ 6.6 Hz). ^{13}C NMR (100 MHz, $CDCl_3$, 27 °C): δ 9.64 ($C_{9,11}$), 45.16 ($C_{8,10}$), 61.98 (C_7), 128.00 (C_4), 129.98 (C_3), 130.87 (C_5), 140.15 (C_6), 146.61 (C_2), 183.49 (C_1). MS (EI, 70 eV, 162 °C): *m/z* (%) 533 (36) [R_2Bi^+], 503 (10) [R_2Bi^+−C_2H_6], 460 (8) [R_2Bi^+−$(C_2H_5)_2NH$], 371 (8) [RBi^+], 209 (10) [Bi^+], 162 (97) [R^+], 91 (100) [$C_7H_7^+$]. FT-Raman (500–50 cm^{-1}; relative intensities in parentheses, strongest = 10): 357 (1.8), 299 (1.8), 267 (1), 229 (8.8), 186 (4), 163 (3.2), 96 (10). FT-IR (cm^{-1}): 471m, 427s, 395m, 385br m, 354m, 231br s, 181s, 165m, 148m, 115m, 87m, 79m, 73s, 63m, 58m.

4.4. Synthesis of [2-(Et_2NCH_2)C_6H_4]$_2$BiBr (**3**)

A solution of 2-(Et_2NCH_2)C_6H_4Br (5 g, 20.6 mmol) in thf (60 ml) was added dropwise to Mg turnings [0.9 g, 37 mmol; activated with 1,2-dibromoethane (1.0 ml)] in thf (20 ml) and then refluxed for 3 h, to give an orange solution The solution of the organomagnesium derivative was filtered to remove unreacted magnesium. A solution of $BiCl_3$ (2.18 g, 6.9 mmol) in thf (70 ml) was added at −20 °C, during 1 h, to the RMgBr solution thus obtained. The reaction mixture was stirred at −20 °C for one more hour and then for 12 h at room temperature, resulting in a clear yellow solution. The solvent was removed and diethyl ether was added to precipitate the insoluble salts. Distilled water was added and the organic phase was separated and dried over anhydrous Na_2SO_4. The Na_2SO_4 was filtered off and washed with diethyl ether. The unified organic phases were concentrated to about 10–12 ml and stored at −28 °C. Colorless crystals (0.645 g), which proved to be **3** and not **1** as expected, precipitated overnight. The solubility of **3** in different organic solvents is similar to that of **2**. Yield: 0.645 g. M.p. 88–89 °C. Anal. Calc. for $C_{22}H_{32}BiBrN_2$: C, 43.08; H, 5.26; N, 4.57. Found: C, 42.85; H, 5.04; N, 4.37%. ^{1}H NMR (400 MHz, $CDCl_3$, 27 °C): δ 1.02t (12H, $H_{9,11}$, $^3J_{HH}$ 7.2 Hz), 2.70q (8H, $H_{8,10}$, $^3J_{HH}$ 7.1 Hz), 3.87s (4H, H_7), 7.37 m (4H, $H_{4,5}$), 7.52m (2H, H_3), 8.56m (2H, H_6). ^{13}C NMR (100 MHz, $CDCl_3$, 27 °C): δ 9.61 ($C_{9,11}$), 45.19 ($C_{8,10}$), 61.98 (C_7), 127.97 (C_4), 129.92 (C_3), 130.92 (C_5), 141.14 (C_6), 146.66 (C_2), 180.30 (C_1). MS (DCI_{pos}, NH_3, 412 °C): *m/z* (%) 613 (32) [M^++H], 533 (31) [R_2Bi^+], 450 (6) [$RBiBr^+$], 164 (100) [R^++2H], 162 (56) [R^+], 91 (16) [$C_7H_7^+$]. MS (DCI_{neg}, NH_3, 199 °C): *m/z* (%) 693 (90) [MH^-+Br], 650 (31) [MH^-+Br−C_2H_5N], 79 (100) [Br^-]. FT-Raman (500–50 cm^{-1}; relative intensities in parentheses, strongest = 10): 359 (2.5), 311 (1.6), 188 (2.6), 150 (2.6), 132 (1), 77 (10). FT-IR (cm^{-1}): 494m, 430s, 391m, 356m, 307m, 252w, 200m, 194m, 186s, 147br s, 136s, 105m, 92m, 85m, 79m.

4.5. Synthesis of [2-(Et_2NCH_2)C_6H_4]$_2$BiI (**4**)

A solution of **2** (1.0 g, 1.7 mmol) in methylene dichloride (20 ml) was mixed with a solution of KI (0.73 g, 4.4 mmol) in distilled water (20 ml). The reaction mixture was stirred for 4 h, then additional distilled water (20 ml) was added and the organic phase was separated. The aqueous phase was washed with CH_2Cl_2 (3 × 15 ml) and the unified organic phases were dried over anhydrous Na_2SO_4. After filtration and removal of the solvent to dryness, the solid residue was washed with hexane leaving a pale yellow powder. Recrystallization from CH_2Cl_2 gave **4** as pale yellow crystals. Yield: 0.94 g (81%). M.p. 113 °C. Anal. Calc. for $C_{22}H_{32}BiIN_2$: C, 40.01; H, 4.88; N, 4.24. Found: C, 39.74; H, 4.53; N, 4.02%. ^{1}H NMR (300 MHz, $CDCl_3$, 20 °C): δ 1.02t (12H, $H_{9,11}$, $^3J_{HH}$ 7.2 Hz), 2.71q (8H, $H_{8,10}$, $^3J_{HH}$ 7.1 Hz), 3.87s (4H, H_7), 7.34dt (2H, H_4, $^3J_{HH}$ 7.3, $^4J_{HH}$ 1.5 Hz), 7.41dt (2H, H_5, $^3J_{HH}$ 7.3, $^4J_{HH}$ 1.5 Hz), 7.51dd (2H, H_3, $^3J_{HH}$ 7.3, $^4J_{HH}$ 1.0 Hz), 8.75d (2H, H_6, $^3J_{HH}$ 6.9 Hz). ^{13}C NMR (75.4 MHz, $CDCl_3$, 20 °C): δ 9.71 ($C_{9,11}$), 45.37 ($C_{8,10}$), 62.16 (C_7), 128.02 (C_4), 129.86 (C_3), 131.22 (C_5), 143.66 (C_6), 146.84 (C_2), 173.98 (C_1). MS (DCI_{pos}, NH_3, 180 °C): *m/z* (%) 661 (100) [M^++H], 533 (100) [R_2Bi^+], 498 (15) [$RBiI^+$], 371 (6) [RBi^+], 325 (9) [R_2H^+], 290 (6) [RI^++H], 164 (100) [R^++2H], 162 (73) [R^+], 91 (17) [$C_7H_7^+$]. MS (DCI_{neg}, NH_3, 207 °C): *m/z* (%) 786 (22) [M^-+I], 127 (100) [I^-]. FT-Raman (500–50 cm^{-1}; relative intensities in parentheses, strongest = 10): 359 (1.3), 185 (2.2), 104 (10), 70 (2.2). FT-IR (cm^{-1}): 488m, 478m, 429s, 400w, 356w, 260m, 251m, 184s, 147m, 108s, 79w, 73s, 63s, 58s.

4.6. Synthesis of [2-(Et_2NCH_2)C_6H_4]$BiCl_2$ (**5**)

A solution of $BiCl_3$ (0.91 g, 2.9 mmol) in diethyl ether (50 ml) is added dropwise to a solution of **1** (1.0 g, 1.45 mmol) in diethyl ether (50 ml). A white precipitate is immediately formed. The reaction mixture is stirred at room temperature for 12 h and then it is filtered. The crude solid is washed with diethyl ether (3 × 20 ml) and dried in vacuum to yield **5** as a white powder. Compound **5** is only slightly soluble in dimethylsulfoxide and is practically insoluble in other common organic solvents. Yield: 1.85 g (97%). M.p. 230 °C (dec.). Anal. Calc. for $C_{11}H_{16}BiCl_2N$: C, 29.88; H, 3.65; N, 3.17. Found: C, 29.65; H, 3.44; N, 3.05%. ^{1}H NMR (300 MHz, DMSO-d_6, 20 °C): δ 1.05t (6H, $H_{9,11}$, $^3J_{HH}$ 7.1 Hz), AB spin system with A at δ 2.95dq (2H, $H_{(8,10)A}$, $^2J_{HH}$ 14.2, $^3J_{HH}$ 7.1 Hz) and B at δ 3.02dq ppm (2H, $H_{(8,10)B}$, $^2J_{HH}$ 14.2, $^3J_{HH}$ 7.1 Hz), 4.42s (2H, H_7), 7.50dt (1H, H_4, $^3J_{HH}$ 7.3, $^4J_{HH}$ 0.8 Hz), 7.76t (1H, H_5, $^3J_{HH}$ 7.2 Hz), 7.94d (1H, H_3, $^3J_{HH}$ 7.4 Hz), 9.17d (1H, H_6, $^3J_{HH}$ 7.3 Hz). ^{13}C NMR (75.4 MHz, DMSO-d_6, 20 °C): δ 9.55 ($C_{9,11}$), 44.19 ($C_{8,10}$), 62.06 (C_7), 128.19 (C_4), 129.97 (C_3), 130.74 (C_5), 138.83 (C_6), 150.93 (C_2), 215.16 (C_1). MS (EI, 70 eV, 245 °C): *m/z* (%) 441 (23) [M^+], 426 (100) [M^+−Me], 406 (85) [$RBiCl^+$], 371 (25) [RBi^+], 341 (5) [RBi^+−C_2H_6], 299 (4) [RBi^+−Et_2N], 209 (46) [Bi^+], 162 (75) [R^+], 91 (95) [$C_7H_7^+$]. FT-Raman (500–50 cm^{-1}; relative intensities in parentheses, strongest = 10): 362 (2), 338 (1.3) 312 (1.3), 243 (10), 216(1.5), 201 (0.8), 177 (2.8), 149 (0.8), 125 (4.8), 110 (2.3), 98 (0.8), 85 (2.3). FT-IR (cm^{-1}): 493m, 477m, 436m, 425s, 397m, 363m, 337br m, 310w, 299w, 251br s, 212m, 206m, 200m, 183br m, 159br m, 148m, 115m, 97m, 92m, 80m.

4.7. Synthesis of [2-(Et_2NCH_2)C_6H_4]$BiBr_2$ (**6**)

A suspension of **5** (0.5 g, 1.13 mmol) in methylene dichloride (20 ml) was stirred vigorously for 24 h with a solution of KBr (0.67 g, 5.6 mmol) in distilled water (30 ml). The reaction mixture was filtered and the precipitate was washed with distilled water (20 ml) and acetone (3 × 10 ml), then dried in vacuum to give **6** as a white powder. Yield: 0.52 g (86%). M.p. 260 °C (dec.). Anal. Calc. for $C_{11}H_{16}BiBr_2N$: C, 24.88; H, 3.04; N, 2.64. Found: C,

24.62; H, 2.81; N, 2.32%. ^{1}H NMR (300 MHz, DMSO-d_6, 20 °C): δ 1.05t (6H, $H_{9,11}$, $^3J_{HH}$ 6.6 Hz), AB spin system with A at δ 3.01dq (2H, $H_{(8,10)A}$, $^2J_{HH}$ 14.2, $^3J_{HH}$ 7.1 Hz) and B at δ 3.08dq ppm (2H, $H_{(8,10)B}$, $^2J_{HH}$ 14.3, $^3J_{HH}$ 7.1 Hz), 4.48s (2H, H_7), 7.53t (1H, H_4, $^3J_{HH}$ 7.1 Hz), 7.75t (1H, H_5, $^3J_{HH}$ 7.0 Hz), 7.96d (1H, H_3, $^3J_{HH}$ 7.1 Hz), 9.31d (1H, H_6, $^3J_{HH}$ 6.6 Hz). ^{13}C NMR (75.4 MHz, DMSO-d_6, 20 °C): δ 10.13 ($C_{9,11}$), 45.09 ($C_{8,10}$), 63.04 (C_7), 128.81 (C_4), 130.46 (C_3), 131.60 (C_5), 140.77 (C_6), 151.85 (C_2), 211.74 (C_1). MS (DCI$_{pos}$, NH_3, 212 °C): *m/z* (%) 532 (11) [M^++H], 452 (38) [$RBiBr^+$], 450 (38) [$RBiBr^+$], 371 (4) [RBi^+], 179 (11) [R^++NH_3], 164 (100) [R^++2H], 91 (8) [$C_7H_7^+$]. MS (DCI$_{neg}$, NH_3, 230 °C): *m/z* (%) 610 (12) [M^-+Br], 531 (38) [M^-], 81 (96) [Br^-], 79 (100) [Br^-]. FT-Raman (500–50 cm^{-1}; relative intensities in parentheses, strongest = 10): 362 (1.4), 341 (1.1), 310 (0.7), 240 (1.4), 212 (1.4), 200 (0.9), 157 (10), 124 (4), 83 (5.7), 71 (1.3). FT-IR (cm^{-1}): 494m, 487m, 483m, 476m, 431s, 424s, 396br m, 361s, 332m, 306m, 291br m, 238s, 215s, 200m, 194m, 174m, 161s, 147m, 118m, 112m, 106m, 98m.

4.8. Synthesis of [2-(Et_2NCH_2)C_6H_4]BiI_2 (**7**)

Similar to **6**, from a suspension of **5** (0.506 g, 1.14 mmol) in diethyl ether (20 ml) and a solution of KI (1.15 g, 6.9 mmol) in distilled water (20 ml). Compound **7** was isolated as a yellow powder, which is more soluble than **5** in methylene chloride, chloroform, DMSO or thf. Yield: 0.62 g (87%). M.p. 220 °C (dec.). Anal. Calc. for $C_{11}H_{16}BiI_2N$: C, 21.14; H, 2.58; N, 2.24. Found: C, 20.78; H, 2.25; N, 2.01%. ^{1}H NMR (300 MHz, DMSO-d_6, 20 °C): δ 1.04t (6H, $H_{9,11}$, $^3J_{HH}$ 7.1 Hz), AB spin system with A at δ 3.063dq (2H, $H_{(8,10)A}$, $^2J_{HH}$ 14.1, $^3J_{HH}$ 7.1 Hz) and B at δ 3.163dq ppm (2H, $H_{(8,10)B}$, $^2J_{HH}$ 14.9, $^3J_{HH}$ 7.8 Hz), 4.52s (2H, H_7), 7.56dt (1H, H_4, $^3J_{HH}$ 7.3, $^4J_{HH}$ 0.9 Hz), 7.67dt (1H, H_5, $^3J_{HH}$ 7.4, $^4J_{HH}$ 0.9 Hz), 7.94d (1H, H_3, $^3J_{HH}$ 7.9 Hz), 9.59d (1H, H_6, $^3J_{HH}$ 5.7 Hz). ^{13}C NMR (75.4 MHz, DMSO-d_6, 20 °C): δ 10.17 ($C_{9,11}$), 45.78 ($C_{8,10}$), 63.47 (C_7), 128.18 (C_4), 129.74 (C_3), 131.90 (C_5), 145.19 (C_6), 151.60 (C_2), 200.30 (C_1). MS (EI, 70 eV, 247 °C): *m/z* (%) 498 (100) [$RBiI^+$], 371 (21) [RBi^+], 341 (3) [RBi^+–C_2H_6], 209 (18) [Bi^+], 162 (21) [R^+], 91 (25) [$C_7H_7^+$]. FT-Raman (500–50 cm^{-1}; relative intensities in parentheses, strongest = 10): 127 (4.1), 111 (10), 70 (6.9). FT-IR (cm^{-1}): 489m, 475m, 427m, 421s, 394w, 359s, 330m, 299m, 287m, 274m, 256m, 234s, 212s, 206m, 200m, 191s, 174m, 159m, 145w, 129s, 118m, 95s, 87s, 80s.

4.9. X-ray structure determination

The details of the crystal structure determination and refinement for compounds **1**–**4** are given in Table 7. Data were collected on Bruker SMART APEX diffractometer by using graphite-monochromated Mo Kα radiation (λ = 0.71073 Å). For this purpose the crystals were attached with epoxy glue on cryoloops and the data were collected at room temperature (297 K). The structures were refined with anisotropic thermal parameters. The hydrogen atoms were refined with a riding model and a mutual isotropic thermal parameter. The Flack parameter for compound **4** is −0.006(7). For structure solving and refinement the software package SHELX-97 was used [58]. The drawings were created with the DIAMOND program [59].

4.10. Computational details for DFT calculations

Quantum-chemical DFT [48] calculations were carried out on the compounds **8**–**14** with the mPW1PW functional [61] using the commercially available suite of programs GAUSSIAN03 (Rev. E1) [62]. Although the use of all-electron basis sets provide better

Table 7
X-ray crystal data and structure refinement for compounds **1**–**4**.

	1	**2**	**3**	**4**
Empirical formula	$C_{33}H_{48}BiN_3$	$C_{22}H_{32}BiClN_2$	$C_{22}H_{32}BiBrN_2$	$C_{22}H_{32}BiIN_2$
Formula weight	695.72	568.93	613.38	660.38
T (K)	297(2)	297(2)	297(2)	297(2)
λ (Å)	0.71073	0.71073	0.71073	0.71073
Crystal system	Cubic	Monoclinic	Triclinic	Orthorhombic
Space group	$Pa\bar{3}$	$C2/c$	$P\bar{1}$	$P2_12_12_1$
Unit cell dimension				
a (Å)	18.6245(8)	23.998(3)	14.276(2)	9.6577(10)
b (Å)	18.6245(8)	15.2355(16)	14.970(2)	13.0522(14)
c (Å)	18.6245(8)	16.3674(17)	19.093(3)	37.325(4)
α (°)	90.00	90	71.227(3)	90
β (°)	90.00	130.192(2)	80.621(3)	90
γ (°)	90.00	90.00	62.713(2)	90
Volume (Å^3)	6460.3(5)	4571.4(9)	3432.8(9)	4705.0(9)
Z	8	8	6	8
D_{calc} (g cm^{-3})	1.431	1.653	1.780	1.865
Absorption coefficient (mm^{-1})	5.482	7.838	9.458	8.815
F(0 0 0)	2800	2224	1776	2512
Crystal size (mm)	0.25 × 0.22 × 0.20	0.28 × 0.24 × 0.21	0.43 × 0.27 × 0.21	0.24 × 0.22 × 0.16
θ Range for data collection (°)	1.89–25.01	2.22–25.00	1.60–25.00	1.90–25.00
Reflections collected	44 772	16 313	25 095	25 006
Independent reflections (R_{int})	1914 (0.0597)	4020 (0.0459)	11 990 (0.0442)	8284 (0.0506)
Data/restraints/parameters	1914/0/114	4020/26/259	11 990/0/726	8284/0/478
Absorption correction	Multi-Scan [60]	Multi-Scan [60]	Multi-Scan [60]	Multi-Scan [60]
Goodness-of-fit on F^2	1.344	1.158	1.030	1.127
Final R indices[a]				
R_1	0.0593	0.0436	0.0434	0.0505
wR_2	0.1069	0.0902	0.0881	0.0901
R indices (all data)				
R_1	0.0608	0.0504	0.0621	0.0562
wR_2	0.1075	0.0931	0.0936	0.0920
Largest difference peak and hole (e Å^{-3})	1.411 and −1.812	0.901 and −1.849	1.128 and −1.263	1.170 and −1.750

[a] $I > 2\sigma(I)$.

accuracy, pseudopotential techniques are useful when relativistic effects have to be taken into account. Thus, the Schäfer, Horn, and Ahlrichs [63] double-ζ plus polarization all-electron basis sets (BS's) were used for C, H, and N, while the LanL2DZ BS with relativistic effective core potentials (RECP) [64] were adopted for the heavier Bi species [65]. The adoption of the LanL2DZ BS for Bi has been chosen due to the good results obtained when applied to similar systems such as monoorganobismuth(III) dihalides containing the 2,6-$[MeN(CH_2CH_2)_2NCH_2]_2C_6H_3$ and 2,6-$(Me_2NCH_2)_2C_6H_3$ pincer ligand [33]. Geometry optimization calculations were performed starting from the structural data, when available, without introducing any symmetry restrain. A pruned (99 590) grid was adopted (Ultrafine grid option) in order to avoid imaginary frequencies. Force constants and the resulting vibrational IR- and Raman-active frequencies were computed by analytically determining the second derivatives of the energy with respect to the Cartesian nuclear coordinates. For all compounds NBO populations [66] and Wiberg bond indexes [50] were calculated at the optimized geometries. The programs GABEDIT 2.0.7 [67] and MOLDEN 4.7 [68] were used to investigate the charge distributions and MO's shapes.

Acknowledgements

Financial support from National University Research Council (Research Project TD-100/2006) and Ministry of Education and Research of Romania (Research Project PNII-ID 2052/2009) is greatly appreciated. We also thank the National Center for X-ray Diffraction (Babes-Bolyai University, Cluj-Napoca, Romania) for support in the solid-state structure determinations. We thank Dr. Alessandra Garau for recording FT-Raman and FT-IR spectra, and Dr. Roberto Bini (LENS, European Laboratory for Non-Linear Spectroscopy, University of Florence) for providing the Bruker IFS120 HR spectrometer.

Appendix A. Supplementary material

CCDC 731957, 731955, 731954 and 731956 contain the supplementary crystallographic data for this paper. These data can be obtained free of charge from The Cambridge Crystallographic Data Centre via www.ccdc.cam.ac.uk/data_request/cif.

Supplementary data (the supplementary material also contains figures representing the molecular structure of compounds **3** and **4**, optical isomers of **1–4**, supramolecular architectures in the crystals of compounds **2–4**, ^{1}H NMR spectrum of **1**, comparative ^{1}H and ^{13}C NMR spectra for compounds **2–4**, comparative ^{1}H NMR spectra for compounds **5–7**, comparative ^{1}H NMR aromatic region for compounds **1–7**, experimental *vs.* simulated AB system for the 8,10-H protons in dihalorganobismuthanes **5–7**, NMR simulation parameters for the AB system in **5** and **7**, optimized geometries in orthogonal Cartesian format calculated for **8**-**10**, $(\mathbf{8})_2$–$(\mathbf{10})_2$ and **11–14**, selected experimental FT-Raman and FT-IR active frequencies for compounds $(\mathbf{8})_2$–$(\mathbf{10})_2$ and **2–7**, experimental FT-Raman and FT-IR spectra of $(\mathbf{8})_2$–$(\mathbf{10})_2$) associated with this article can be found, in the online version, at doi:10.1016/j.jorganchem.2010.01.004.

References

[1] H. Suzuki, Y. Matano (Eds.), Organobismuth Chemistry, Elsevier Science B.V, Amsterdam, 2001.
[2] G.G. Briand, N. Burford, Chem. Rev. 99 (1999) 2601.
[3] P.J. Sadler, H. Li, H. Sun, Coord. Chem. Rev. 185–186 (1999) 689.
[4] S. Schulz, Coord. Chem. Rev. 215 (2001) 1.
[5] E.R.T. Tiekink, Crit. Rev. Oncol. Hemat. 42 (2002) 217.
[6] C. Limberg, Angew. Chem., Int. Ed. 42 (2003) 5932.
[7] M. Mehring, Coord. Chem. Rev. 251 (2007) 974.
[8] S.-F. Yin, J. Maruyama, T. Yamashita, S. Shimada, Angew. Chem., Int. Ed. 47 (2008) 6590.
[9] B. Murray, J. Hvoslef, H. Hope, P.P. Power, Inorg.Chem. 22 (1983) 3421.
[10] H.J. Breunig, R. Rösler, E. Lork, Angew. Chem., Int. Ed. 37 (1998) 3175.
[11] H. Althaus, H.J. Breunig, R. Rösler, E. Lork, Organometallics 18 (1999) 328.
[12] H.J. Breunig, H. Althaus, Phosphorus, Sulfur Silicon 168 (2001) 123.
[13] H.J. Breunig, I. Gheşner, E. Lork, J. Organomet. Chem. 664 (2002) 130.
[14] L. Balázs, H.J. Breunig, E. Lork, Organometallics 21 (2002) 2584.
[15] B. Twamley, C.D. Sofield, M.M. Olmstead, P.P. Power, J. Am. Chem. Soc. 121 (1999) 3357.
[16] N.J. Hardman, B. Twamley, P.P. Power, Angew. Chem., Int. Ed. 39 (2000) 2771.
[17] Y. Wang, B. Quillian, X.-J. Yang, P. Wei, Z. Chen, C.S. Wannere, P.v.R. Schleyer, G.H. Robinson, J. Am. Chem. Soc. 127 (2005) 7672.
[18] R. Wolf, J. Fischer, R.C. Fischer, J.C. Fettinger, P.P. Power, Eur. J. Inorg. Chem. (2008) 2515.
[19] H.J. Breunig, N. Haddad, E. Lork, M. Mehring, C. Mügge, C. Nolde, C.I. Raţ, M. Schürmann, Organometallics 28 (2009) 1202.
[20] T. Sasamori, Y. Arai, N. Takeda, R. Okazaki, Y. Furukawa, M. Kimura, S. Nagase, N. Tokitoh, Bull. Chem. Soc. Jpn. 75 (2002) 661.
[21] N. Tokitoh, Y. Arai, R. Okazaki, S. Nagase, Science 277 (1997) 78.
[22] X.-W. Li, J. Lorberth, W. Massa, S. Wocadlo, J. Organomet. Chem. 485 (1995) 141.
[23] E.V. Avtomonov, X.-W. Li, J. Lorberth, J. Organomet. Chem. 530 (1997) 71.
[24] T. Sasamori, N. Takeda, N. Tokitoh, Chem. Commun. (2000) 1353.
[25] T. Sasamori, N. Takeda, M. Fujio, M. Kimura, S. Nagase, N. Tokitoh, Angew. Chem., Int. Ed. 41 (2002) 139.
[26] T. Sasamori, E. Mieda, N. Takeda, N. Tokitoh, Angew. Chem., Int. Ed. 44 (2005) 3717.
[27] T. Sasamori, E. Mieda, N. Tokitoh, Bull. Chem. Soc. Jpn. 80 (2007) 2425.
[28] Y. Yamamoto, X. Chen, K. Akiba, J. Am. Chem. Soc. 114 (1992) 7906.
[29] S. Yoshida, M. Yasui, F. Iwasaki, Y. Yamamoto, X. Chen, K. Akiba, Acta Crystallogr., Sect. B 50 (1994) 151.
[30] X. Chen, Y. Yamamoto, K. Akiba, Heteroatom Chem 6 (1995) 293.
[31] Y. Yamamoto, K. Ohdoi, X. Chen, M. Kitano, K. Akiba, Organometallics 12 (1993) 3297.
[32] H.J. Breunig, L. Königsmann, E. Lork, N. Philipp, M. Nema, C. Silvestru, A. Soran, R.A. Varga, R. Wagner, Dalton Trans. (2008) 1831. and references cited therein.
[33] A. Soran, H.J. Breunig, V. Lippolis, M. Arca, C. Silvestru, Dalton Trans. (2009) 77.
[34] L. Dostál, I. Císařová, R. Jambor, A. Růžička, R. Jirásko, J. Holeček, Organometallics 25 (2006) 4366.
[35] L. Dostál, P. Novák, R. Jambor, A. Růžička, I. Císařová, R. Jirásko, J. Holeček, Organometallics 26 (2007) 2911.
[36] L. Balázs, H.J. Breunig, E. Lork, C. Silvestru, Eur. J. Inorg. Chem. (2003) 1361.
[37] L. Balázs, O. Stângă, H.J. Breunig, C. Silvestru, Dalton Trans. (2003) 2237.
[38] E.J. Fernández, A. Laguna, J.M. López-de-Luzuriaga, M. Monge, M. Nema, M.E. Olmos, J. Pérez, C. Silvestru, Chem. Commun. (2007) 571.
[39] J. Emsley, Die Elemente, Walter de Gruyter, Berlin, 1994.
[40] S. Kamepalli, C.J. Carmalt, R.D. Culp, A.H. Cowley, R.A. Jones, N.C. Norman, Inorg. Chem. 35 (1996) 6179.
[41] K. Akiba (Ed.), Chemistry of Hypervalent Compounds, Wiley-VCH, New York, 1999.
[42] The N–X–L nomenclature system has been previously described: N valence shell electrons about a central atom X with L ligands. C.W. Perkins, J.C. Martin, A.J. Arduengo III, W. Lau, A. Alegria, K. Kochi, J. Am. Chem. Soc. 102 (1980) 7753.
[43] J. Rigauy, S.P. Klesney (Eds.), Nomenclature of Organic Chemistry – The Blue Book, Pergamon Press, Oxford, 1979.
[44] C.J. Carmalt, A.H. Cowley, R.D. Culp, R.A. Jones, S. Kamepalli, N.C. Norman, Inorg. Chem. 36 (1997) 2770.
[45] K.H. Whitmire, D. Labahn, H.W. Roesky, M. Noltemeyer, G.M. Sheldrick, J. Organomet. Chem. 402 (1991) 55.
[46] K.H. Ebert, R.E. Schulz, H.J. Breunig, C. Silvestru, I. Haiduc, J. Organometal. Chem. 470 (1994) 93.
[47] S.C. James, N.C. Norman, A.G. Orpen, J. Chem. Soc., Dalton Trans. (1999) 2837.
[48] (a) W. Koch, M.C. Holthausen, A Chemist's Guide to Density Functional Theory, 2nd ed., Wiley-VCH, Weinheim, 2002;
(b) F. Neese, Coord. Chem. Rev. 253 (2009) 526.
[49] A.P. Soran, C. Silvestru, H.J. Breunig, G. Balázs, J.C. Green, Organometallics 26 (2007) 1196.
[50] K. Wiberg, Tetrahedron 24 (1968) 1083.
[51] J. Moilanen, C. Ganesamoorthy, M.S. Balakrishna, H.M. Tuononen, Inorg. Chem. 48 (2009) 6740.
[52] M.C. Aragoni, M. Arca, F. Demartin, F.A. Devillanova, F. Lelj, F. Isaia, V. Lippolis, A. Mancini, L. Pala, G. Verani, Eur. J. Inorg. Chem. (2004) 3099.
[53] (a) A.J. Blake, F.A. Devillanova, R.O. Gould, W.-S. Li, V. Lippolis, S. Parsons, C. Radek, M. Schröder, Chem. Soc. Rev. 27 (1998) 195;
(b) M.C. Aragoni, M. Arca, F. Demartin, F.A. Devillanova, A. Garau, F. Isaia, F. Lelj, V. Lippolis, G. Verani, Chem. Eur. J. 7 (2001) 3122;
(c) M.C. Aragoni, M. Arca, A.J. Blake, F.A. Devillanova, W.-W. du Mont, A. Garau, V. Lippolis, G. Verani, Angew. Chem., Int. Ed. 40 (2001) 4229;
(d) M.C. Aragoni, M. Arca, F. Demartin, F.A. Devillanova, A. Garau, F. Isaia, V. Lippolis, G. Verani, Dalton Trans. (2005) 2252;
(e) C.G. Hrib, F. Rithe, E. Seppälä, M. Bächer, C. Druckenbrodt, C. Wismach, P.J. Jones, W.-W. du Mont, V. Lippolis, F.A. Devillanova, M. Bül, Eur. J. Inorg. Chem. (2006) 88;
(f) M. Arca, M.C. Aragoni, F.A. Devillanova, A. Garau, F. Isaia, V. Lippolis, A. Mancini, G. Verani, Bioinorg. Chem. Appl. 1 (2006), doi:10.1155/BCA/2006/58937.

[54] MestReC and MestReNova, Mestrelab Research S.L., A Coruña 15706, Santiago de Compostela.
[55] MASPEC II Data System, Mass Spectrometry Services Ltd., M25 9WB Manchester.
[56] C.M. Wehman-Ooyevaar, I.F. Luitwieler, K. Vatter, D.M. Grove, W.J.J. Smeets, E. Horn, L.A. Spek, G. van Koten, Inorg. Chim. Acta 252 (1996) 55.
[57] L. Soran, V. Coman, A. Soran, C. Silvestru, Cent. Eur. J. Chem. 2 (2004) 563.
[58] G.M. Sheldrick, Acta Crystallogr., Sect. A 64 (2008) 112.
[59] K. Brandenburg, DIAMOND – Visual Crystal Structure Information System, Release 3.1d, Crystal Impact GbR, Bonn, Germany, 2006.
[60] G.M. Sheldrick, SADABS, Program for Area Detector Adsorption Correction, University of Göttingen, Germany, 1996.
[61] C. Adamo, V. Barone, J. Chem. Phys. 108 (1998) 664.
[62] GAUSSIAN 03, Revision E.01, M.J. Frisch, G.W. Trucks, S.H.B. chlegel, G.E. Scuseria, M.A. Robb, J.R. Cheeseman, J.A. Montgomery Jr., T. Vreven, K.N. Kudin, J.C. Burant, J.M. Millam, S.S. Iyengar, J. Tomasi, V. Barone, B. Mennucci, M. Cossi, G. Scalmani, N. Rega, G.A. Petersson, H. Nakatsuji, M. Hada, M. Ehara, K. Toyota, R. Fukuda, J. Hasegawa, M. Ishida, T. Nakajima, Y. Honda, O. Kitao, H. Nakai, M. Klene, X. Li, J.E. Knox, H.P. Hratchian, J.B. Cross, V. Bakken, C. Adamo, J. Jaramillo, R. Gomperts, R.E. Stratmann, O. Yazyev, A.J. Austin, R. Cammi, C. Pomelli, J.W. Ochterski, P.Y. Ayala, K. Morokuma, G.A. Voth, P. Salvador, J.J. Dannenberg, V.G. Zakrzewski, S. Dapprich, A.D. Daniels, M.C. Strain, O. Farkas, D.K. Malick, A.D. Rabuck, K. Raghavachari, J.B. Foresman, J.V. Ortiz, Q. Cui, A.G. Baboul, S. Clifford, J. Cioslowski, B.B. Stefanov, G. Liu, A. Liashenko, P. Piskorz, I. Komaromi, R.L. Martin, D.J. Fox, T. Keith, M.A. Al-Laham, C.Y. Peng, A. Nanayakkara, M. Challacombe, P.M.W. Gill, B. Johnson, W. Chen, M.W. Wong, C. Gonzalez, J.A. Pople, Gaussian, Inc., Wallingford CT, 2004.
[63] A. Schäfer, H. Horn, R.J. Ahlrichs, J. Chem. Phys. 97 (1992) 2571.
[64] (a) T.H. Dunning Jr., P.J. Hay, in: H.F. Schaefer III (Ed.), Methods of Electronic Structure, Theory, Vol. 2, Plenum Press, New York, 1977;
(b) J.V. Ortiz, P.J. Hay, R.L. Martin, J. Am. Chem. Soc. 114 (1992) 2736.
[65] (a) Basis sets obtained from Basis Set Exchange and Basis Set EMSL Library. D.J. Feller, J. Comput. Chem. 17 (1996) 1571;
(b) K.L. Schuchardt, B.T. Didier, T. Elsethagen, L. Sun, V. Gurumoorthi, J. Chase, J. Li, T.L. Windus, J. Chem. Inf. Model. 47 (2007) 1045.
[66] (a) A.E. Reed, F. Weinhold, J. Chem. Phys. 83 (1985) 1736;
(b) A.E. Reed, L.A. Curtiss, F. Weinhold, Chem. Rev. 88 (1988) 899.
[67] GABEDIT is a free Graphical User Interface for computational chemistry packages. It is written by Abdul-Rahman Allouche. GABEDIT is available from http://lasim.univ-lyon1.fr/allouche/gabeditb.
[68] G. Schaftenaar, J.H. Noordik, J. Comput.-Aided Mol. Des. 14 (2000) 123.